Measurement of Forces between Galactomannan Polymer Chains: Effect of Hydrogen Bonding

Yu Cheng*,† and Robert K. Prud'homme*

Department of Chemical Engineering, Princeton University, Princeton, New Jersey 08544

John Chik and Donald C. Rau

Laboratory of Physical and Structural Biology, National Institutes of Child Health and Human Development, National Institutes of Health, Bethesda, Maryland 20892-0924

Received June 7, 2002; Revised Manuscript Received October 24, 2002

ABSTRACT: Packing free energies and structural transitions of concentrated arrays of guar galactomannan macromolecules and of guars modified by hydroxypropyl substitution (HPG) have been studied using the osmotic stress method combined with X-ray scattering. All show a liquid crystalline structure with packing free energies that are very similar for guar and HPG and well described by the model of Selinger and Bruinsma for entropic steric repulsion between chains. In addition, a transition from the liquid crystalline form to a crystalline structure is observed as native guar becomes more densely packed. This transition is related to the propensity of guar to form intermolecular hydrogen bonds in solutions. Hydroxypropyl substitution of galactomannan hydroxyl groups causes steric interference that decreases the stability of this hydrogen-bonded crystalline structure. Even for moderately hydroxypropyl-substituted guar (∼0.3 HP/sugar residue), the transition occurs at a much higher osmotic pressure than for native guar. The extra work needed to crystallize this HPG compared with guar is calculated to be 3 kT/mannose unit or 6−7 kT per hydroxypropyl group. No transition was found for more highly substituted guars. Urea increased the osmotic pressure necessary for the transition of guar but also resulted in new crystalline packing structure.

Introduction

Guar galactomannan is a water-soluble polysaccharide derived from the endosperms of a leguminuous plant, *Cyamopsis tetragonalobush*. It is widely used in many industrial applications such as oil recovery,[1,2] food,[3,4] and personal care[5] to control solution viscoelastic properties. The structure of guar is shown in Figure 1a: it has a linear backbone of β-1,4-linked mannose units with α-1,6-linked galactose units randomly attached as side chains. The ratio of mannose to galactose is ∼1.6−1.8:1.[6]

Guar can form both inter- and intramolecular hydrogen bonds. Its crystalline structure has been determined in the relative humidity (RH) range of 40−80%. The mannose backbone and galactose side chains form antiparallel planar sheets as shown schematically in Figure 1b. An extensive network of both direct sugar−sugar and water-mediated hydrogen bonds within and between sheets stabilizes the structure. The distance between mannose backbones within the sheet is about 4.5 Å. The distance between the stacked sheets is about 16 Å.[7−10] In dilute aqueous solution, guar exists as a random coil.[11] However, rheological properties of guar solution depart from those of typical "random coil" polysaccharides and display much higher viscosities at the same dimensionless concentration. This is believed to be due to the intermolecular association of mannose backbones in regions sparsely substituted with galactose side chains.[12] The solution properties of galactomannan polymers have been studied extensively.[11−15] However, the role of hydrogen bonding and network structure in guar solutions is still not firmly established.

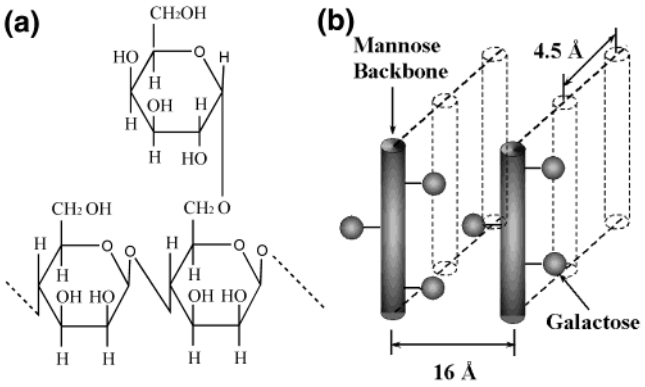

Figure 1. (a) Structure of guar: guar has a linear backbone of β-1,4-linked mannose units with α-1,6-linked galactose units randomly attached as side chains. The ratio of mannose to galactose is 1.6−1.8:1. (b) Schematic representation of the crystalline structure of guar: guar chains pack into antiparallel sheets. The intersheet distance is about 16 Å, and the distance between guar backbones inside the sheet is approximately 4.5 Å.

Our goal in this paper is to develop a further understanding of galactomannan interactions in concentrated guar solutions, i.e., the relative contributions of repulsive (such as hydration forces and steric exclusion) and attractive (hydrogen-bonding and van der Waals interactions) forces. We have directly measured the mean thermodynamic force between polymer chains as a function of intermolecular spacing by the osmotic stress technique. In brief, an ordered array of macromolecules is equilibrated against a bathing solution of a polymer of known osmotic pressure that is excluded from the

* Authors to whom correspondence should be addressed. Y.C.: e-mail yu_cheng@merck.com; R.K.P.: e-mail prudhomm@princeton.edu.

† Current address: Merck Research Laboratories, WP78-304, West Point, PA 19486.

10.1021/ma020887e CCC: $22.00
Published on Web 11/27/2002

macromolecular phase. The intermolecular spacing between macromolecules is then determined by Bragg scattering of X-rays.[16] This technique has been used to measure the intermolecular forces in various systems such as lipid bilayers,[17,18] DNA double helixes,[19,20] rigid polysaccharides,[21] and proteins.[22,23]

The osmotic stress method offers an opportunity to relate the directly measured molecular interactions to macroscopic solution properties. By integrating the experimental osmotic pressure vs distance (volume) curve, changes in interaction free energy can be calculated from the work required to bring two macromolecular chains together:[20,24]

$$\Delta W = \int \mathrm{d}W = -\int \Pi_{\mathrm{osm}}\, \mathrm{d}V \qquad (1)$$

Furthermore, measuring the osmotic pressure vs distance curve at different temperatures or solute activities makes it possible to calculate changes in entropy and enthalpy or in solute binding of the system.[24]

Native guar can be modified by grafting different side groups onto the sugar hydroxyl groups. Hydroxypropyl guar (HPG) is the most widely used guar derivative.[25] Stoichiometric control of the propylene oxide substitution on the guar chain results in HPGs with various degrees of substitutions. By comparing the force curve for guar and HPGs, we probe the effect of bulky hydroxypropyl substitutions on the intermolecular interactions.

The structure of the presentation is as follows. The materials and experimental techniques are given in section 2. In section 3, the results are presented first for hydroxypropyl guar (HPG), for which the osmotic stress vs intermolecular distance follows the predictions of theories of liquid crystalline polymers interacting through steric repulsion of undulating chains. We then investigate a transition of native guar from a liquid crystalline to crystalline form with increasing osmotic stress. In the next section, a lightly substituted hydroxypropyl guar (HPG) is studied. By comparing the transition for this HPG vs native guar, we calculate the energy required to overcome the steric hindrance and loss of hydrogen bonding due to hydroxypropyl group substitution. Finally, the addition of urea to guar solutions is shown to change the crystal structure, and this is discussed in terms of the role of bridging waters of hydration for these polysaccharide polymers.

2. Experimental Section

2.1. Materials. Native guar galactomannan was provided by Rhodia (Cranbury, NJ) as a gift. Three HPG samples were obtained from Halliburton Co. (Duncan, OK) with different molar substitution (MS) levels: MS = 0.3, 1.07, and 1.53. The addition of hydroxypropyl groups to guar is described by the molar substitution, which is defined as the average number of moles of hydroxypropyl groups substituted per mole of anhydro sugar units. It is a measure of the total number of moles of propylene oxide that have been added to the guar polymer chain. Both guar and HPGs were degraded by acid hydrolysis to a lower molecular weight range (MW ~ 100 000) and then dissolved in 10 mM TrisCl (pH 8.0), 2 mM EDTA at a concentration of 1% (w/w). The degradation procedure has been described in detail elsewhere.[26]

2.2. Osmotic Stress. The method for direct force measurement by osmotic stress has been described in detail by Parsegian et al.[16] The general idea of the experiment is quite simple (Figure 2). Condensed macromolecular arrays are equilibrated against a bathing polymer solution, typically poly(ethylene glycol), PEG, of known osmotic pressure. It is often not necessary to enforce separation between the macromolecular phase and PEG solution with a semipermeable dividing membrane since many macromolecules phase separate from PEG solutions. Water and small solutes are free to exchange between the PEG and guar phases. After equilibrium is achieved, the osmotic pressures in both the polymer and macromolecular phases are the same, as necessarily are the chemical potentials of all the permeating species. If the condensed macromolecular phase is sufficiently ordered, the intermolecular distance can be determined as a function of the applied PEG stress by Bragg scattering of X-rays. The dependence of osmotic pressure on the concentration and MW of PEG has been measured directly using a vapor pressure osmometer, and the pressure data can be found on the World Wide Web: http://mecko.nichd.nih.gov/Lpsb/docs/OsmoticStress.html.

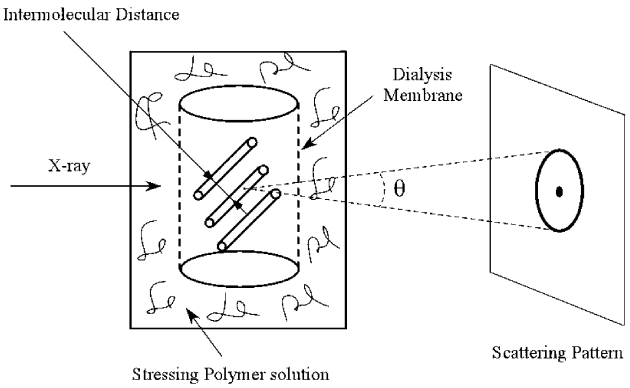

Figure 2. Scheme of the osmotic stress method. An ordered array of macromolecules is equilibrated against a solution of a polymer that is excluded from the condensed array. If necessary, the exclusion can be enforced using a semipermeable membrane to separate the two phases. At equilibrium, the osmotic pressure applied by the stressing polymer solution is balanced by the repulsive force between macromolecules in the condensed phase. The spacing between macromolecules can be determined by Bragg scattering of X-rays. Scattering from the stressing polymer solution is typically much weaker than from the ordered array.

Condensed guar and HPG arrays were formed by slow dialysis in a Pierce Microdialysis System 500 cell with a 1000 MW cutoff membrane (Spectrum Laboratories, Inc., CA) against PEG (MW ~ 8000, Sigma Chemical Co.) aqueous solutions that varied between 30 and 53 wt %. These pellets were then cut into pieces approximately 2 × 2 × 0.5 mm. Since guar and HPG remain phase-separated from PEG solutions more concentrated than ~20 wt %, the pellets were directly equilibrated against PEG (MW 8000 or 20 000) solutions for another 2 weeks with one change of bathing solution after 1 week. No differences in stress vs separation spacing curves for guar and the HPG samples were observed between PEG 8000 and 20 000 molecular weights, confirming that PEG is excluded from the ordered array. To achieve higher osmotic pressures ($\Pi > 10^7$ Pa), guar samples were equilibrated against water vapor in equilibrium with saturated salt solutions.[27,28] Osmotic pressure is related to the relative humidity, RH, through[16]

$$\Pi = -\frac{kT}{v_{\mathrm{w}}} \ln(\mathrm{RH}) = -\frac{kT}{v_{\mathrm{w}}} \ln(p/p_0) \qquad (2)$$

where p is the vapor pressure of the saturated salt solution, p_0 is the vapor pressure of pure water, and v_{w} is the molecular volume of water.

2.3. X-ray Scattering Measurements. Distances between polymer chains are determined by Bragg X-ray scattering using an Enraf-Nonius Service Corp. (Bohemia, NY) fixed copper anode Diffractis 601 X-ray generator (National Institutes of Health, Bethesda, MD). The camera design and imaging system have been described in detail elsewhere.[29] Guar and HPG pellets were sealed with a small amount of

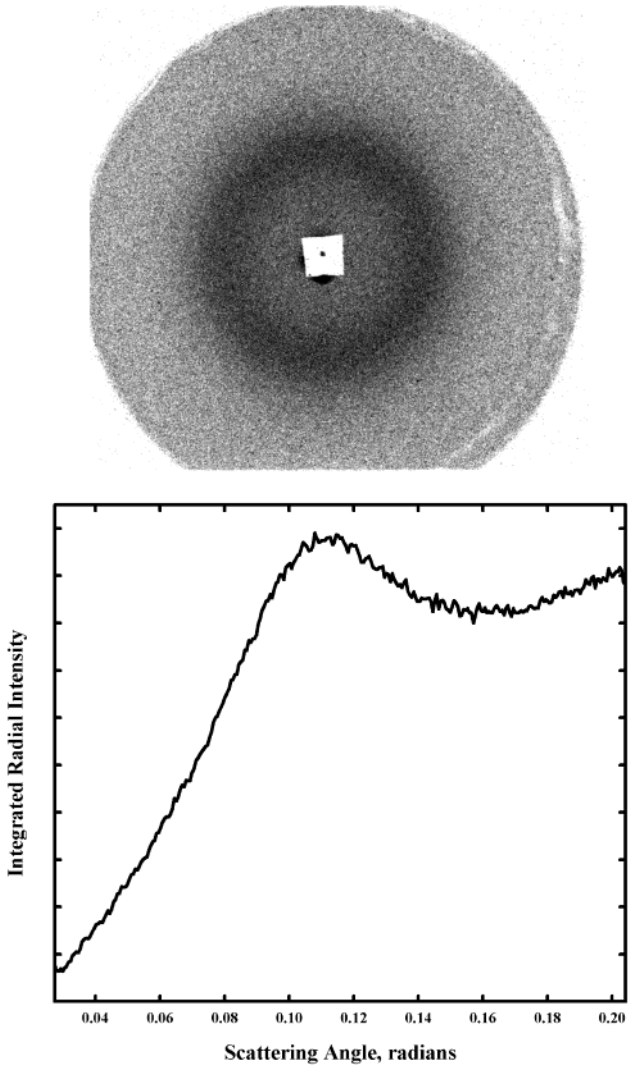

Figure 3. (a) Typical X-ray diffraction powder pattern for condensed ordered arrays of HPG with MS 1.53. (b) Plot of the integrated radial intensity, corresponding to the diffraction pattern, as a function of the scattering angle.

equilibrating solution in the sample cell and then mounted into a temperature-controlled holder at 20 °C. The specially designed X-ray cell has been previously reported.[30] Diffraction patterns from guar and HPG samples were recorded by direct exposure of Fujifilm BAS image plates and digitized with a Fujifilm BAS 2500 scanner. The images were analyzed using the National Institutes of Health Image software and SigmaPlot 7.0 (SPSS Inc.). Mean pixel intensities between scattering radii $r - 0.05$ mm and $r + 0.05$ mm averaged over all azimuthal angles of the powder pattern diffraction, $\langle I(r)\rangle$, were used to calculate integrated radial intensity profiles, $2\pi r\langle I(r)\rangle$.

Results and Discussion

3.1. Forces in the Liquid Crystalline Packing Regime of HPG and Guar. A typical diffraction pattern seen for condensed ordered arrays of HPG with MS 1.07 and 1.53 over the entire osmotic pressure range studied ($\sim 10^{5.5}-10^{8.5}$ Pa) and for native guar and HPG with MS 0.3 at lower stresses is shown in Figure 3 along with a plot of the radially integrated intensity shown as a function of scattering radius. A single broad peak is observed with no indication of a second-order reflection. Since the Bragg spacing corresponding to the peak decreases as the osmotic pressure of the bathing PEG solution increases, we take this scattering to reflect an

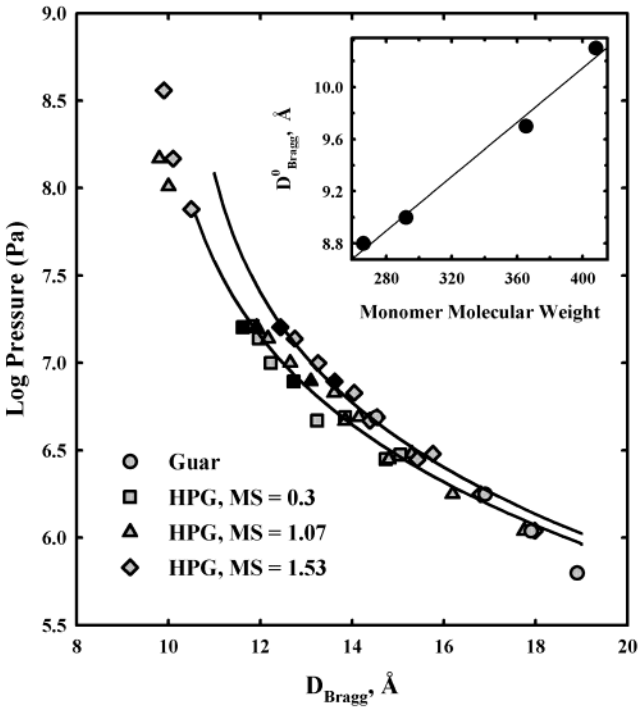

Figure 4. Osmotic pressure vs Bragg spacing data for guar and HPG samples in the liquid crystalline regime. The curve fit is based on prediction of Selinger and Bruinsma[34] for simple steric repulsion of flexible chains in a LC form (eq 4), with $n = {}^2/_3$. Black and gray symbols stand for experiments at 5 and 20 °C, respectively. Inset: the dry polymer rod diameter spacing, D^0_{Bragg}, calculated from the power law fit given in eq 4 with $n = {}^2/_3$, correlates well with the monomeric molecular weight of the polymer. The monomeric molecular weights are 266 (guar), 292 (HPG MS 0.3), 365.3 (HPG MS 1.07), and 408 (HPG MS 1.53).

average distance between macromolecular chains in a nematic liquid crystalline structure.

Figure 4 shows the dependence of the Bragg spacing on osmotic stress in the liquid crystalline regime for the four samples investigated. The thermodynamic force curves show little sensitivity to the degree of hydroxypropyl molar substitution or to temperature. The apparent exponential decay length of the guar and HPG force curves is about 2 Å. This is significantly smaller than the 3.5 Å decay length seen previously for hydration or water structuring forces between the much more rigid carbohydrates xanthan (a charged double helix) and schizophyllan (an uncharged triple helical polysaccharide).[21] Bragg reflection peaks for the latter two polysaccharides were also much narrower than for the HPG and guar samples. The polymer persistence length, L_p, of guar is only ~4 nm compared with ~120 nm for xanthan and ~200 nm for schizophyllan. Given the higher flexibility and the broader reflection peaks, we have analyzed the HPG and guar liquid crystalline data using the model of Stelinger and Bruinsma,[34] which considers steric repulsions between chains arising from fluctuations in configurations, i.e., an entropic repulsion. The free energy per unit length, $\Delta F/L$, due to steric repulsion between semiflexible chains in a confined space has the following form:[34,35]

$$\frac{\Delta F}{L} \sim \frac{C}{(D_{\text{Bragg}} - D^0_{\text{Bragg}})^n} \qquad (3)$$

D^0_{Bragg} is the Bragg spacing between dry polymer chains,

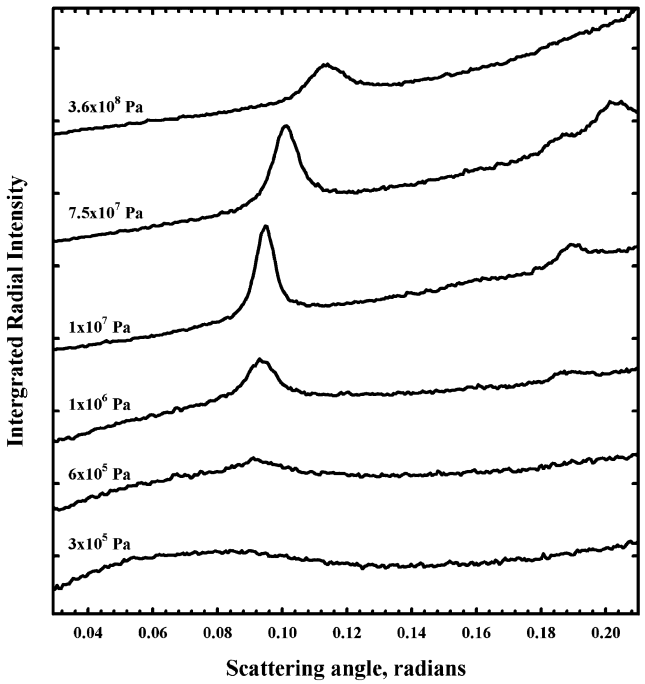

Figure 5. Integrated radial intensity profiles for the X-ray scattering powder patterns of guar solutions at various osmotic pressures.

i.e., the diameter of the polymer rod. C and n are constants. For commonly found hexagonal packing of repulsive chains, $n = {}^2/_3$. The osmotic pressure

$$\Pi = -\frac{\mathrm{d}\Delta F}{\mathrm{d}V} = -\frac{\mathrm{d}(\Delta F/L)}{D_{\mathrm{Bragg}}\,\mathrm{d}D_{\mathrm{Bragg}}} = \frac{nC}{D_{\mathrm{Bragg}}(D_{\mathrm{Bragg}} - D^0_{\mathrm{Bragg}})^{n+1}} \quad (4)$$

The $n = {}^2/_3$ power law form provides a good fit to the experimental data with the fitting parameter $D^0_{\mathrm{Bragg}} \sim$ 9.7 Å for HPG (MS 1.07) and 10.3 Å for HPG (MS 1.53) (Figure 4). These diameters are consistent with the apparent hard wall seen at $\Pi \sim 10^{8.5}$ Pa (~10% relative humidity). The more limited pressure data from the LC form of guar and HPG (MS 0.3) can also be well fit to the power law form, yielding D^0_{Bragg} values of 8.8 and 9 Å, respectively. The polymer rod diameter D^0_{Bragg} grows as more substituent groups are added to the polymer backbone; a good correlation between D^0_{Bragg} and the monomeric molecular weight of guar and different HPGs was obtained (Figure 4 inset). Assuming cylindrical chain packing and a length of 5 Å/ monomer along the carbohydrate chain, then the observed slope, $\Delta D/\Delta M$, corresponds to a reasonable density of 0.9 g/mL for the hydroxypropyl moiety. The interaction free energy of HPG and guar is dominated at these close spacings by the entropy loss due to the steric repulsion of undulating chains.

3.2. Guar Galactomannan. Both the guar and HPG (MS 0.3) samples show a transition from the liquid crystalline regime to a different packing geometry at higher pressures. Figure 5 shows the integrated radial intensity profiles of the scattering patterns of native guar at different osmotic pressures. At low osmotic pressure (3 atm) there is a very broad, diffuse powder-pattern ring, characteristic of the liquid crystalline form. As the osmotic pressure increases, a sharp scattering peak develops on top of the broad peak while the intensity of the broad peak decreases. At 100 atm, the broad LC peak totally disappears with only the sharp scattering ring left. This peak is narrow with a Bragg spacing of approximately 16 Å and has clear second-order reflection at half this distance. At even wider scattering angles, we have also observed a sharp scattering peak with a $D_{\mathrm{Bragg}} \sim 4.5$ Å for the same sample (data not shown). These distances are consistent with the previously reported guar crystalline lattice, suggesting that guar crystallizes into a sheet structure at high osmotic pressures, with the ~4.5 Å peak corresponding to the distance between mannose backbones within a mannose sheet and the 16 Å reflection to the distance between sheets (Figure 1b). The crystalline structure of guar with its interchain hydrogen bonds and backbone interactions is more stable than the LC form at these high packing densities. At $\sim 10^{8.5}$ Pa the crystalline peak is weakened and significantly broadened, and the second-order reflection begins to disappear. The removal of these ordered water molecules induces disorder, confirming the importance of these waters in stabilizing the crystalline state.

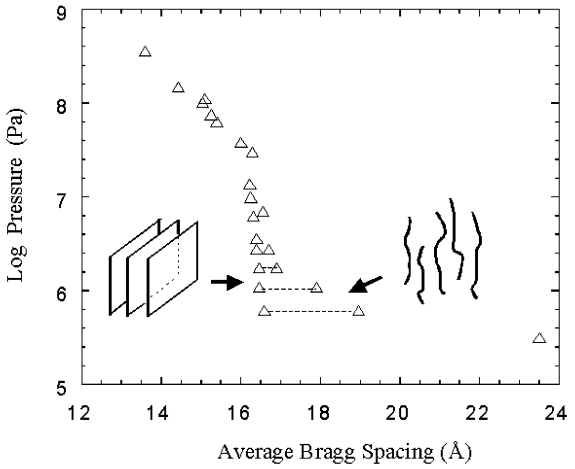

Figure 6. Pressure vs distance curve for condensed guar arrays. As osmotic pressure increases, there is a transition from liquid crystalline to crystalline structure. At these high packing densities, the crystalline form of guar is more stable due to intermolecular hydrogen bonding and stacked backbones.

Figure 6 plots the osmotic pressure Π as a function of the average Bragg spacing obtained from X-ray scattering. The data show a transition between crystalline and LC structures at 20 °C. This might be caused by kinetic limitations, a distribution of interfacial packing energies between scattering domains, or a heterogeneous distribution of galactose on the guar backbone.[31] Within the crystalline regime, Bragg spacings are insensitive to osmotic pressure changes in the range of 10^6–$10^{7.5}$ Pa, indicative of a deep energy well between the guar crystalline sheets, i.e., attractive forces. At pressures above $\sim 10^{7.5}$ Pa, D_{Bragg} begins to decrease. It has been shown that there are water molecules bridging guar chains in the sheet structure that are important for the formation and stability of the crystalline structure.[7] At very high pressures, these associated water molecules are removed and the chains move closer.

Since the LC and crystalline form have different geometries, we plot log Π as a function of the volume per mannose unit along the polymer backbone in Figure 7. For the LC structure, we assume a hexagonal packing

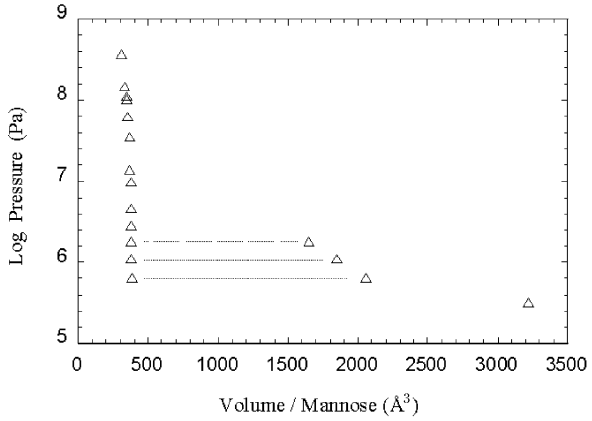

Figure 7. Osmotic pressure is plotted as a function of volume per mannose unit along the backbone, assuming hexagonal packing of the condensed guar arrays. The volume per mannose decreases substantially across the LC−crystalline transition.

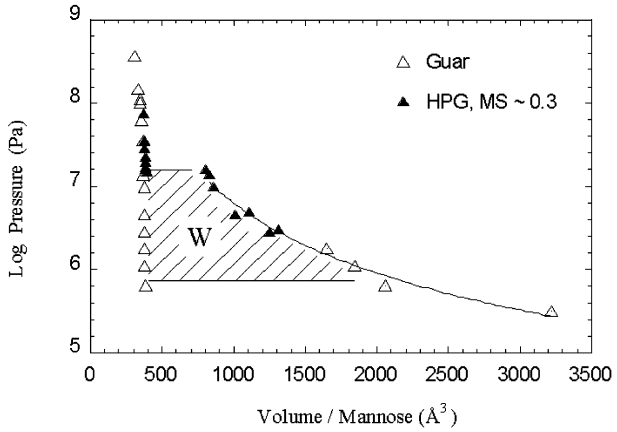

Figure 8. Pressure−volume data are shown for guar and HPG (MS ∼ 0.3) to characterize the transition from the liquid crystalline to crystalline structures. Compared with guar, the transition occurs at much higher pressures for HPG. The shaded area shows the difference in $P-V$ work done on guar and HPG in the packing transition from liquid crystalline to crystalline forms.

characteristic of repulsive polymer chains. The length of a mannose unit along the backbone was taken to be 5 Å. The volume/mannose unit can be then calculated as

$$V_{\mathrm{LC}}[\text{Å}^3] = 5(2/\sqrt{3})D_{\mathrm{Bragg}}{}^2 \qquad (5)$$

For the crystalline forms of fenugreek,[9] lucerne,[9] and guar galactomannans,[36] the spacings both along the mannose backbone (∼5 Å) and between the mannose backbones (∼4.5 Å) have been observed insensitive to relative humidity compared with the ∼16 Å spacing between mannose backbones within a sheet. The volume/mannose unit is then

$$V_{\mathrm{C}}[\text{Å}^3] = 5 \times 4.5 \times D_{\mathrm{Bragg}} \qquad (6)$$

The volume per mannose unit decreases dramatically from 1650 to 380 Å^3 in the LC-to-crystalline transition. Subsequent dehydration of the crystalline form (to $10^{8.5}$ Pa) results in the loss of another ∼70 Å^3, corresponding to ∼2−3 waters/ mannose.

3.3. Hydroxypropyl Guar (Moderately Substituted, MS ∼ 0.3). A packing transition is also observed for the HPG sample with a low MS value (∼0.3). The osmotic pressure vs volume/mannose plot is shown in Figure 8. The result for guar is also included as a comparison. Only broad liquid crystalline peaks are seen for this HPG up to ∼10^7 Pa. Both a broad LC peak and a much sharper peak analogous to the crystalline form of unmodified guar, however, are observed at $10^{7.2}$ Pa. At pressures higher than $10^{7.4}$ Pa, the sharp scattering peak dominates. At even higher pressures, the Bragg spacing of the apparent HPG crystalline form changes in parallel with that for native guar but is ∼0.3−0.5 Å larger. The same apparent transition from the LC to crystalline transition occurs for this HPG but at a much higher osmotic stress than for native guar. The crystalline form of HPG is energetically less favorable than of native guar, likely due to the steric hindrance effect introduced by hydroxypropyl substitution and the disruption of the geometry of inter- and intrasheet hydrogen bonds. We can estimate how much more work is required to compress HPG chains into crystalline sheets than to compress guar, by integrating the pressure−volume curve between the two structural transitions. This additional work is illustrated in the shaded area in Figure 8. By choosing the transition point as the pressure at which the liquid crystalline and crystalline peaks have about equal intensities, ∼$10^{7.2}$ Pa for HPG and ∼$10^{5.8}$ Pa for guar, the $P\Delta V$ work was calculated to be approximately 3 kT/mannose unit.

A MS of 0.3 means that, on average, there are 0.3 hydroxypropyl groups added per sugar unit. Assuming the galactose/mannose ratio of 0.5 for guar, then each monomeric unit along the mannose backbone has approximately 0.45 hydroxypropyl groups. Therefore, the total energy change per hydroxypropyl substitution is 6−7 kT (∼20 kJ mol^{-1}). This energy can be compared to the energy of a hydrogen bond (14−20 kJ mol^{-1}).[32] Given these large energies, it is not surprising that no liquid crystalline−crystalline packing transition was observed for the HPG samples with much higher MS values (1.07 and 1.53).

3.2. Effect of Urea. Urea is a known denaturant and structure breaker in many biological systems. It has been shown that urea can break the intermolecular hydrogen bonding between polysaccharides chains.[37] We have, therefore, examined the effect of urea on the structure and intermolecular interactions of guar in these concentrated arrays. Figure 9 shows scattering profiles as the concentration of urea is increased at a constant osmotic stress of ∼$10^{7.7}$ Pa. Without urea, guar shows the typical crystalline peak with a distance about 16 Å. With the addition of urea, the intensity of the sharp crystalline peak decreases in intensity and broadens in width. At 3 M urea concentration, an additional peak develops at a higher scattering radius. At 6 M urea, the original guar crystalline peak disappears, leaving only the guar−urea peak. This peak has a Bragg spacing of about 13.8 Å. The narrow reflection is completely different from the broad scattering peak characteristic of the LC form. This suggests that urea is able to disrupt the original guar structure. Urea, however, is incorporated with guar chains into a new crystalline structure. The structure of this new crystalline form warrants further investigation.

In Figure 10, we fix the urea concentration at 6 M but vary the PEG osmotic stress. We have assumed for simplicity in calculating the volume of the new guar−urea structure that it is isomorphous with the guar crystalline structure and that only the spacing within

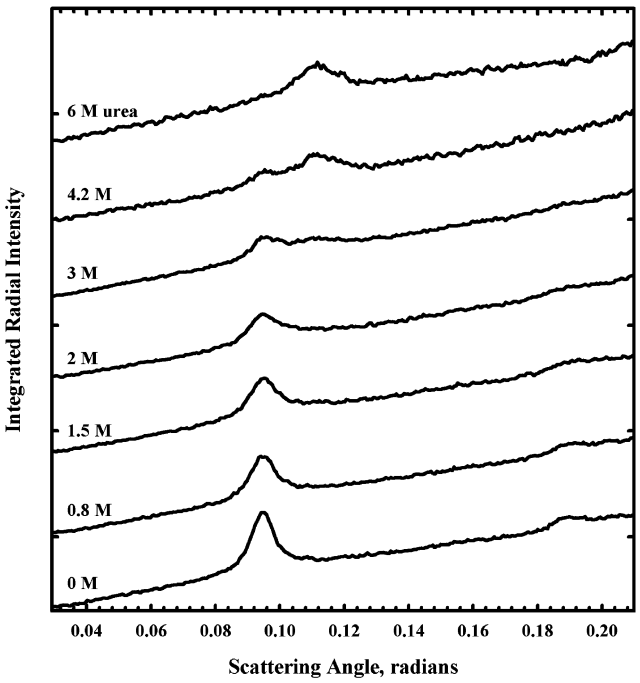

Figure 9. Integrated radial intensity profiles for the X-ray scattering powder patterns of guar solutions at fixed osmotic pressure ($10^{6.7}$ Pa) but different urea concentrations.

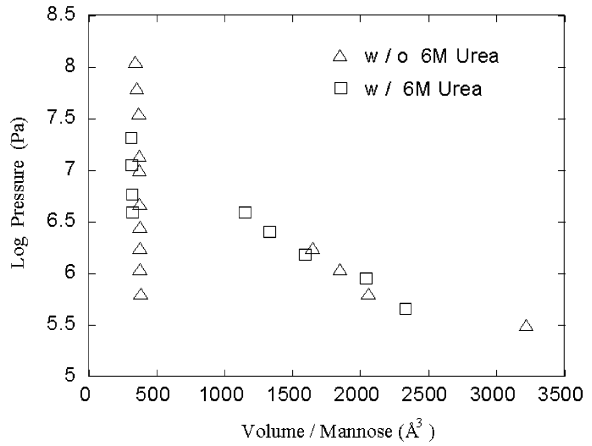

Figure 10. Pressure−volume data are shown for guar solutions with and without the addition of 6 M urea. Under low osmotic pressures, urea disrupts intermolecular hydrogen bonding and the guar crystalline structure. As the pressure increases, however, a different crystalline structure of guar is formed that incorporates urea.

the galactose−mannose plane is affected by incorporation of urea. Only a transition from liquid crystalline packing with broad reflection peaks to the new guar−urea crystalline peak is observed. The guar crystalline peak is not observed over the range of osmotic pressures. The data for guar arrays without urea are also included for comparison. There is little apparent effect of urea on the pressure−volume dependence in the LC form. Repulsive interactions are still dominated by simple steric forces. This does not exclude direct interactions of urea with guar in the LC structure. The transition to the new guar−urea crystalline form occurs at a much higher pressure than the transition in the absence of urea. Therefore, under low osmotic pressures, 6 M urea does disrupt the intermolecular hydrogen bonding and the native guar crystalline structure. However, as the pressure increases, urea seems able to hydrogen bond with guar chains and form a new, densely packed crystalline structure.

4. Discussion and Conclusions

In this study, the mean force between native guar and HPG chains has been directly measured as a function of intermolecular spacing by the osmotic stress method combined with X-ray scattering. We have shown that the osmotic stress technique can be applied to moderately flexible polysaccharides polymers, whereas most previous studies have been on much stiffer, helical DNA, xanthan, or schizophyllan. The study demonstrates the ability of the technique to observe and quantify subtle features of steric forces and hydrogen bonding that dominate interactions between most polysaccharide macromolecules. We have been able to obstruct normal interchain associations by introducing hydroxypropyl groups, which sterically block hydrogen bonding.

For the hydroxypropyl guar (HPG) with substitution levels greater than 0.4, the data show liquid crystalline order in the HPG solutions. The intermolecular force vs distance results are consistent with the predictions of Selinger and Bruinsma for polymer chains that interact through steric repulsion of fluctuating chains. At closer spacings, these entropic interactions decay with an apparent length scale of approximately 2 Å, which is significantly different from the 3.5 Å decay length observed for DNA, xanthan, and schizophyllan systems. Water structuring or repulsive hydration forces are believed to dominate the close interactions of these latter systems.[19−21] The very broad Bragg scattering peaks of guar and HPG in the LC regime compared with the other much stiffer macromolecules are also consistent with substantially more chain entropy.

For the native guar at pressures around 10^6 Pa, a transition from liquid crystal to crystal is observed. The reflections observed are consistent with the crystalline structure observed for oriented guar fibers at 40−80% RH. The transition is driven by the ability of guar to form direct or water-mediated hydrogen bonds between mannose and galactose units and, therefore, release hydrating water. At exceedingly high osmotic stress, above $10^{7.5}$ Pa, a further compaction of the crystal structure is observed; the volume per mannose backbone unit decreases from ∼380 to 310 Å^3 (∼2 water molecules). This volume decrease is likely associated with removal of 2−3 bound water molecules that are known to mediate several hydrogen bonds between sugar hydroxyl units in the crystal unit cell.

For moderately substituted guars (MS ∼ 0.3), the LC to crystal transition occurs at much higher pressure compared to that of native guar. The extra work that is required to crystallize HPG is calculated to be 3 kT/mannose unit and 6−7 kT/hydroxypropyl group. This is the extra work required to crystallize the guar which has sterically blocked hydrogen-bonding sites. This is the first technique that allows quantification of these cooperative hydrogen-bonding interactions.

The effect of urea on the structure and intermolecular interactions between guar chains is also studied. At low osmotic pressures, 6 M urea disrupts intermolecular hydrogen bonding and the guar crystalline structure. However, as the pressure increases, urea interacts with guar to form a new crystalline structure, which has not been previously reported. The exact structure of this new crystal form warrants further study.

There are several practical implications and questions for future research that arise from this study. First, we

have demonstrated that the technique can be used to measure interactions in a wide range of other polysaccharide and carbohydrate polymers. The uniformity of hydroxypropyl and carboxymethyl substitution of cellulose as well as modified starch could be explored. In addition, the rate of hydration of guar and HPG is crucial in several of its industrial applications such as hydraulic fracturing in the oil industry. It is interesting that the traditional guar powders used in this application had a molar substitution of hydroxypropyl groups of 0.48. It is above the threshold of 0.3 that we found was the approximate boundary between polymers that crystallized during dehydration in contrast to those that dried into a more poorly ordered liquid crystalline form. The implications of this for the rate of rehydration and dissolution of guar and HPG powders could now be addressed systematically using the osmotic stress technique. It is unknown whether the new guar structure with urea replacing bridging water molecules has different dissolution characteristics. While the role of the relatively small hydroxypropyl group to sterically hinder hydrogen bonding has been demonstrated, it would be of interest to investigate both bulkier and charged ionic groups.

Acknowledgment. We acknowledge financial support from the National Science Foundation under Award NSFBES-9711781.

References and Notes

(1) Prudhomme, R. K.; Constien, V.; Knoll, S. *Adv. Chem. Ser.* **1989**, *89*.
(2) Cheng, Y.; Prud'homme, R. K. *Biomacromolecules* **2000**, *1*, 782.
(3) Fox, J. E. In *Thickening and Gelling Agents for Food*; Imeson, A., Ed.; Blackie Academic Professional: New York, 1997; p 262.
(4) Whistler, R. L.; BeMiller, J. N. *Industrial Gums: Polysaccharides and Their Derivatives;* Academic Press: San Diego, CA, 1993.
(5) Brode, G. L.; Goddard, E. D.; Harris, W. C.; et al. In *Cosmetic and Pharmaceutical Applications of Polymers*; Gebelein, C. G., Cheng, T. C., Yang, V. C., Eds.; Plenum: New York, 1991; p 117.
(6) McCleary, B. V.; Matheson, N. K. *Adv. Carbohydr. Chem. Biochem.* **1986**, *44*, 147.
(7) Chandrasekaran, R.; Bian, W.; Okuyama, K. *Carbohydr. Res.* **1998**, *312*, 219.
(8) Chandrasekaran, R.; Radha, A.; Okuyama, K. *Carbohydr. Res.* **1998**, *306*, 243.
(9) Song, B. K.; Winter, W. T.; Taravel, F. R. *Macromolecules* **1989**, *22*, 2641.
(10) Marchessault, R. H.; Buleon, A.; Deslandes, Y.; et al. *J. Colloid Interface Sci.* **1979**, *71*, 375.
(11) Robinson, G.; Ross-Murphy, S. B.; Morris, E. R. *Carbohydr. Res.* **1982**, *107*, 17.
(12) Morris, E. R.; Cutler, A. N.; Ross-Murphy, S. B.; et al. *Carbohydr. Polym.* **1981**, *1*, 5.
(13) Launay, B.; Cuvelier, G.; Martinez-Reyes, S. *Carbohydr. Polym.* **1997**, *34*, 385.
(14) Goycoolea, F. M.; Morris, E. R.; Gidley, M. J. *Carbohydr. Polym.* **1995**, *27*, 69.
(15) Gittings, M. R.; Cipelletti, L.; Trappe, V.; et al. *J. Phys. Chem. B* **2000**, *104*, 4381.
(16) Parsegian, V. A.; Rand, R. P.; Fuller, N. L.; et al. *Methods Enzymol.* **1986**, *127*, 400.
(17) LeNeveu, D. M.; Rand, R. P.; Parsegian, V. A. *Nature (London)* **1976**, *259*, 601.
(18) Rand, R. P.; Parsegian, V. A. *Biochim. Biophys. Acta* **1989**, *988*, 351.
(19) Podgornik, R.; Rau, D. C.; Parsegian, V. A. *Macromolecules* **1989**, *22*, 1780.
(20) Rau, D. C.; Parsegian, V. A. *Biophys. J.* **1992**, *61*, 246.
(21) Rau, D. C.; Parsegian, V. A. *Science* **1990**, *249*, 1278.
(22) Leikin, S.; Rau, D. C.; Parsegian, V. A. *Nat. Struct. Biol.* **1995**, *2*, 205.
(23) Leikin, S.; Rau, D. C.; Parsegian, V. A. *Proc. Natl. Acad. Sci. U.S.A.* **1994**, *91*, 276.
(24) Leikin, S.; Rau, D. C.; Parsegian, V. A. *Phys. Rev. A* **1991**, *44*, 5272.
(25) Gulbis, J.; Hodge, R. M. In *Reservoir Stimulation*; Economides, M. J., Nolte, K. G., Eds.; John Wiley & Sons: Chichester, England, 2000.
(26) Cheng, Y.; Brown, K. M.; Prud'homme, R. K. *Biomacromolecules* **2002**, *3*, 456.
(27) Seborg, G.; Stamm, A. *Ind. Eng. Chem.* **1931**, *23*, 1273.
(28) Stokes, R. H.; Robinson, R. A. *Ind. Eng. Chem.* **1949**, *41*, 2013.
(29) Kuznetsova, N.; Rau, D. C.; Parsegian, V. A.; et al. *Biophys. J.* **1997**, *72*, 353.
(30) Mudd, C. P.; Tipton, H.; Parsegian, A. V.; et al. *Rev. Sci. Instrum.* **1987**, *58*, 2110.
(31) McCleary, B. V.; Clark, A. H.; Dea, I. C. M.; et al. *Carbohydr. Res.* **1985**, *139*, 237.
(32) Vinogradov, S. N.; Linnel, R. H. *Hydrogen Bonding;* Van Nostrand Reinhold: New York, 1971.
(33) Cheng, Y.; Brown, K. M.; Prud'homme, R. K. *Biomacromolecules* **2002**, *3*, 456.
(34) Selinger, J. V.; Bruinsma, R. F. *Phys. Rev. A* **1991**, *43*, 2910.
(35) Helfrich, W.; Harbich, W. *Chem. Scr.* **1985**, *25*, 32.
(36) Palmer, K. J.; Ballantyne, M. *J. Am. Chem. Soc.* **1950**, *72*, 736.
(37) McQueenmason, S.; Cosgrove, D. J. *Proc. Natl. Acad. Sci. U.S.A.* **1994**, *91*, 6574.

MA020887E